

Figure 6. UV-visible spectra of $\text{MnCl}_{12}\text{TMPS}$ (full lines) and $[\text{MnCl}_{12}\text{TMPS-PVPMe}^+][\text{TsO}^-]$ (dotted lines) in Vaseline.

(from 497 to 490 nm) as expected for the coordination of a nitrogen-containing ligand to a manganese porphyrin.²⁵

Preparation of $[(n\text{-Bu})_4\text{N}]\text{HSO}_5$. Tetra-*n*-butylammonium monoperoxysulfate was prepared from the potassium salt using the procedure published by Trost et al. with some modifications.²⁶ A 2.0-g sample of potassium monoperoxysulfate (6.5 mmol) in 20 mL of water was stirred with 2.0 g of tetra-*n*-butylammonium hydrogen sulfate (5.9 mmol) for 20 min. Then the solution was extracted with 40 mL of dichloromethane. This organic phase was dried over magnesium sulfate and filtered out. After evaporation, the remaining paste was washed with 10 mL of hexane and dried under vacuum. After evaporation, 0.5 g of $[(n\text{-Bu})_4\text{N}]\text{HSO}_5$ was

(25) Kelly, S. L.; Kadish, K. M. *Inorg. Chem.* **1982**, *21*, 3631–3639.

(26) Trost, B. M.; Braslau, R. *J. Org. Chem.* **1988**, *53*, 532–537.

obtained with a purity better than 90% (determined by iodometric titration). **Caution:** this peroxide should be considered as potentially explosive, and despite the repeated number of safe syntheses, we never overpassed this preparation scale.

Typical Procedure for Cyclooctene Epoxidations Catalyzed by Supported Manganese Porphyrin Complexes. A 5-mL flask was loaded with 3 mL of dichloromethane, 20 μL of cyclooctene (154 μmol), 20 μL of 1,2-dichlorobenzene (178 μmol) as internal standard for GC analyses, and 2 μmol of sulfonated manganese porphyrin loaded on 100 mg of PVP (or 2 μmol of sulfonated manganese porphyrin for \sim 250 mg of loaded and protonated or methylated PVP resin). At time zero, 165 mg of PhIO (750 μmol) was added to the stirred reaction mixture. At different reaction times the stirring was stopped to allow the uptake of an aliquot of 1 μL , which was directly analyzed by GC. Concentrations of cyclooctene and cyclooctene oxide were determined after their corresponding response factors. Results described in Figure 5 were obtained starting with 500 μL of cyclooctene (3850 μmol).

Typical Procedure for Adamantane Hydroxylations Catalyzed by Supported Manganese Porphyrin Complexes. A 10-mL flask was loaded with 525 mg of adamantane (3.86 mmol), 120 mg of 1,4-dibromobenzene (internal standard), 1 μmol of the supported catalyst, and 7 mL of dichloromethane (1 μmol of the supported catalyst equals a loading of 1 μmol of $\text{MnCl}_{12}\text{TMPS}$ for 100 mg of PVP in the case of $[\text{MnCl}_{12}\text{TMPS-PVP}]$, or for \sim 250 mg of $[\text{MnCl}_{12}\text{TMPS-PVPMe}^+][\text{TsO}^-]$ or $[\text{MnCl}_{12}\text{TMPS-PVPMe}^+][\text{TsO}^-]$). At time zero, 165 mg of PhIO (750 μmol) was added to the stirred reaction mixture at room temperature under air (results were not modified when performed in an argon atmosphere). Aliquots of 1 μL were directly analyzed by GC. Concentrations of 1-adamantanol, 2-adamantanol, and adamantanone were determined after their corresponding response factors.

Acknowledgment. This work was supported by a "Stimulation" grant from the EEC, including a postdoctoral fellowship for S.C. (on leave from Prs. G. Modena and F. Di Furia laboratory, Padova University). Dr. Anne Robert is gratefully acknowledged for fruitful discussions throughout this work and interpretations of NMR spectra. We are indebted to two referees for detailed remarks and comments.

Contribution from the Department of Chemistry, United States Naval Academy, Annapolis, Maryland 21402, Department of Chemistry and Biochemistry, University of Delaware, Newark, Delaware 19716, and Department of Chemistry, The Catholic University of America, Washington, D.C. 20064

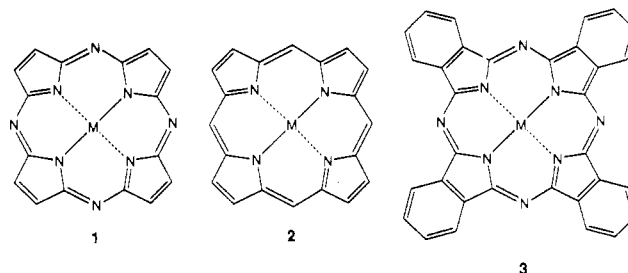
Iron Octaethyltetraazaporphyrins: Synthesis, Characterization, Coordination Chemistry, and Comparisons to Related Iron Porphyrins and Phthalocyanines

Jeffrey P. Fitzgerald,^{*,†} Brian S. Haggerty,[‡] Arnold L. Rheingold,[‡] Leopold May,[§] and Gregory A. Brewer[§]

Received January 31, 1992

This paper describes the synthesis and characterization of a series of iron octaethyltetraazaporphyrin complexes and a comparison of these substances to related iron porphyrins and phthalocyanines. Experimental evidence provided by magnetic susceptibility measurements, ¹H NMR, EPR, and Mössbauer spectroscopies, cyclic voltammetry, and/or X-ray crystallography indicates the tetraazaporphyrin ligand is a stronger σ donor and π acceptor than is a porphyrin ligand. Due to its high σ basicity, the tetraazaporphyrin ligand stabilizes the unusual $S = 3/2$ spin state for iron in chloroiron(III) octaethyltetraazaporphyrin. Yet the high π acidity of the tetraazaporphyrin ligand shifts iron III/II redox potentials 400 mV positive of those for analogous iron porphyrins. In this sense, the tetraazaporphyrin macrocycle is more like a phthalocyanine than a porphyrin. Compared to phthalocyanines, octaethyltetraazaporphyrins are readily soluble. The high solubility, unusual metal spin states, and positively shifted redox potentials of octaethyltetraazaporphyrins suggest that they may have better or unique catalytic properties than porphyrins or phthalocyanines.

Tetraazaporphyrins (**1**), also known as porphyrazines, are a class of aromatic, macrocyclic ligands composed of four pyrrole rings bridged by aza nitrogen atoms. These molecules may be considered to be structural hybrids of the well-studied porphyrins (**2**) (four pyrrole rings connected by methine carbon atoms) and phthalocyanines (**3**) (four isoindole rings bridged by aza nitrogen atoms). As such, tetraazaporphyrins provide an excellent op-



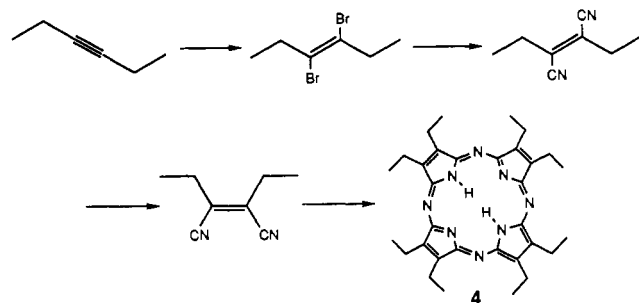
[†] United States Naval Academy.

[‡] University of Delaware.

[§] The Catholic University of America.

portunity to explore the subtle effects of ligand structure on the properties of coordinated metal ions in porphyrinic complexes.

Scheme I



In addition, tetraazaporphyrins show several unique properties (optical, electrochemical, and catalytic) which make them of interest in their own right.

Despite the structural similarities, tetraazaporphyrins are virtually unstudied compared to the related macrocycles, most probably due to the lack of an efficient synthesis of soluble derivatives. Octaphenyltetraazaporphyrins, first reported by Linstead over 50 years ago,¹ have received scattered attention.² In our hands, the poor solubility of these complexes in organic solvents has made it extremely difficult to obtain analytically pure samples.³ Despite considerable effort by Linstead, no great improvement was made in tetraazaporphyrin synthesis or solubility over the next 40 years.⁴ More recently, Schramm and Hoffman have published a general, high-yield route to octakis(alkylthio)tetraazaporphyrins.⁵ While readily soluble, the eight electron-donating thioether groups on the macrocycle periphery certainly alter the electronic properties of this interesting ligand, thus making comparisons to porphyrins and phthalocyanines less meaningful.

We recently reported the facile conversion of alkynes into alkyl- and/or aryl-substituted fumaronitriles and maleonitriles.⁶ These dinitriles serve as a rich source of starting materials for cyclocondensations into soluble alkyl- and/or aryl-substituted tetraazaporphyrins. Octaethyltetraazaporphyrin (4), which is readily prepared from 3-hexyne as outlined in Scheme I, is particularly useful due to its high symmetry and excellent solubility characteristics.

Because of their biological relevance and wealth of comparative data, tetraazaporphyrin complexes of iron have been the focus of our initial efforts. We report herein the synthesis and characterization of several iron octaethyltetraazaporphyrins (5–9). The electronic structures of 5–9 have been examined by magnetic susceptibility measurements, Mössbauer and EPR spectroscopies, and/or cyclic voltammetry. In addition, the X-ray crystal structure of the chloroiron(III) complex (8) has been determined; this is the second tetraazaporphyrin and the first iron tetraazaporphyrin to be so characterized. Selected aspects of the coordination chemistry and redox properties of these iron tetraazaporphyrins are reported and compared to those of related porphyrins and phthalocyanines.

Results and Discussion

Synthesis. Synthetic routes to tetraazaporphyrins have changed little since Linstead's¹ and Fischer's⁷ initial discoveries. Of these two methods, Linstead's cyclocondensation of fumaronitrile and/or

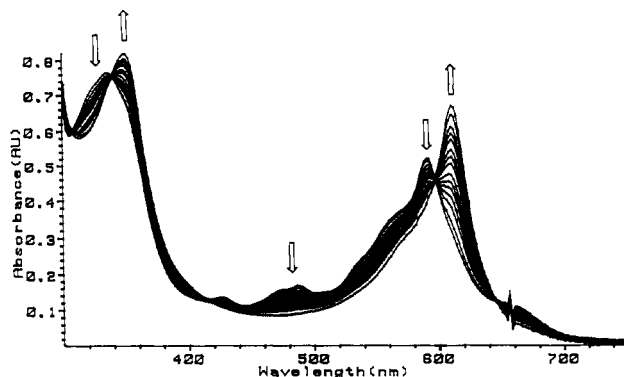


Figure 1. Visible spectrum for the reaction of Fe(OETAP) (5) with O₂ in benzene. Time between scans = 5–20 s.

maleonitrile derivatives is preferred due to its higher yields and fewer steps.

Iron insertion into the metal-free octaethyltetraazaporphyrin (4) and the coordination chemistry of the resulting product are outlined in Scheme II. Heating a toluene/THF solution of 4 in the presence of iron(II) iodide and the hindered base 2,6-lutidine gives iron(II) octaethyltetraazaporphyrin, Fe(OETAP) (5). This four-coordinate compound has been characterized by magnetic susceptibility measurements as having an intermediate-spin ($S = 1$) ground state. As expected for a 14-electron metal complex, 5 has a high affinity for ligands; it will reversibly bind 2 equiv of sterically unhindered ligand, either pyridine or 1-methylimidazole, to produce the diamagnetic, six-coordinate adducts 6a and 6b.

Exposure of 5 to air results in rapid, irreversible oxidation to a μ -oxo dimer, [Fe(OETAP)]₂O (7). This reaction proceeds without detectable intermediates, as indicated by the isosbestic changes in the visible spectrum, shown in Figure 1. Antiferromagnetic coupling of unpaired spins through the oxo bridge gives 7 a diamagnetic ¹H NMR spectrum in which diastereotopic methylene hydrogens clearly indicate the inequivalence of the two tetraazaporphyrin faces. The μ -oxo dimer (7) on treatment with aqueous HCl is converted into chloroiron(III) octaethyltetraazaporphyrin, Fe(OETAP)Cl (8). Magnetic susceptibility measurements, Mössbauer and EPR spectra, and an X-ray crystal structure indicate 8 is an unusual, intermediate ($S = 3/2$) spin complex. Stirring a benzene solution of 8 over aqueous OH⁻ results in re-formation of the dimer (7). Analogous to the four-coordinate iron(II) derivative, 8 binds 2 equiv of added nitrogenous base (with displacement of the chloride ligand) to give a low spin, six-coordinate ferric complex, 9.

There is some question in the literature as to whether treatment of iron(II) phthalocyanine with aqueous HCl in the presence of air produces chloroiron(III) phthalocyanine or an iron(II) phthalocyanine hydrochloride salt (presumably by protonating one of the bridging aza nitrogen atoms).⁸ Accordingly, we initially wondered whether 8 was an iron(II) octaethyltetraazaporphyrin hydrochloride salt. Preparation of 8 by an acid-free method, one-electron oxidation of 5 with Ag⁺, followed by treatment with a quaternary ammonium chloride, proves that 8 is not a hydrochloride salt.

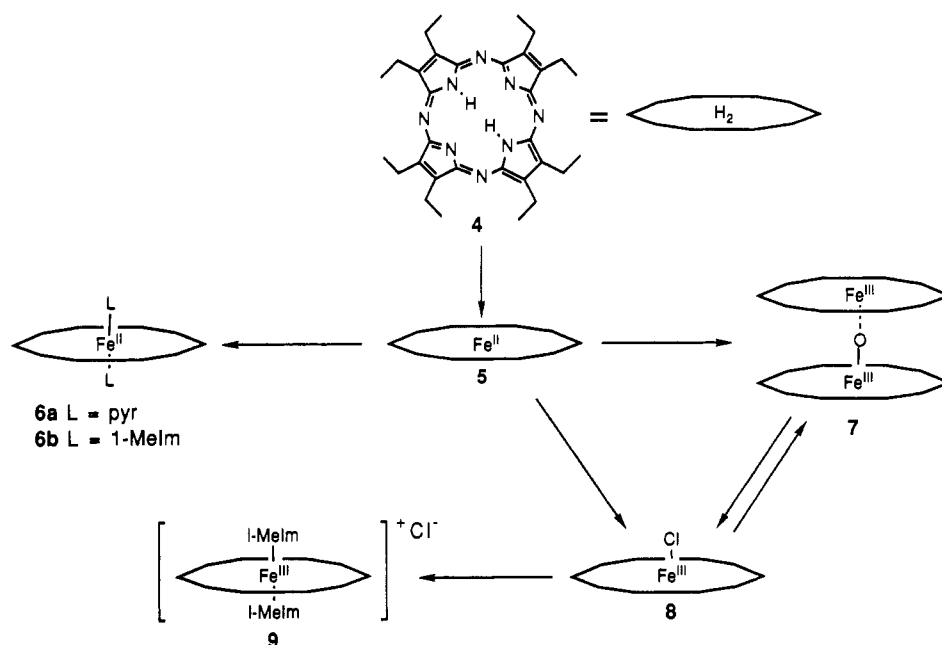
Other than the $S = 3/2$ spin state of Fe(OETAP)Cl (8), the reaction chemistry described above for iron octaethyltetraazaporphyrin is qualitatively very similar to that of simple iron porphyrins and, where comparisons are possible, to that of iron phthalocyanine.

Iron(II) Derivatives. (a) Characterization. Given its high affinity for axial ligands, there was some question whether 5 was a "bare", four-coordinate iron tetraazaporphyrin or a six-coordinate bis-THF complex. Both complexes are known in the case of iron(II) tetraphenylporphyrin⁹ while, in the case of iron(II)

- (1) Cook, A.; Linstead, R. *J. Chem. Soc.* **1937**, 929–933.
- (2) (a) Pitt, D.; Smyth, D. *J. Chem. Phys.* **1958**, *63*, 582–587. (b) Blackburn, E.; Timmons, C. *J. Chem. Soc.* **1970**, 175–178. (c) Svetkina, E.; Filippova, T.; Blyumberg, É.; Kopanenkov, V. *Kinet. Catal.* **1985**, *25*, 935–938. (d) Camenzind, M.; Hill, C. *Inorg. Chim. Acta* **1985**, *99*, 63–67. (e) Stuzhin, P.; Latos-Grazynski, L.; Jezierski, A. *Transition Met. Chem. (London)* **1989**, *14*, 341–346.
- (3) Baakegard, K. Unpublished results, U.S. Naval Academy.
- (4) (a) Linstead, R.; Whalley, M. *J. Chem. Soc.* **1952**, 4839–4846. (b) Ficken, G.; Linstead, R. *J. Chem. Soc.* **1952**, 4846–4854. (c) Baguley, M.; France, H.; Linstead, R.; Whalley, M. *J. Chem. Soc.* **1955**, 3521–3525.
- (5) Schramm, C.; Hoffman, B. *Inorg. Chem.* **1980**, *19*, 383–385.
- (6) Fitzgerald, J.; Taylor, W.; Owen, H. *Synthesis* **1991**, 686–688.
- (7) Fischer, H.; Endermann, F. *Justus Liebigs Ann. Chem.* **1937**, *531*, 245–250.

- (8) (a) Barrett, P.; Frye, D.; Linstead, R. *J. Chem. Soc.* **1938**, 1157–1163. (b) Jones, J.; Twigg, M. *Inorg. Chem.* **1969**, *8*, 2120–2123. (c) Dickens, L. Ph.D. Thesis, Clemson University, Dec 1974; Chapter 2.

Scheme II



phthalocyanine, only the four-coordinate complex has been reported.¹⁰ The elemental analysis of **5** is more consistent with four-coordinate Fe(OETAP). The differences between the calculated percent compositions of the two possibilities are well within detectable limits. The ¹H NMR spectrum of **5** shows only two signals, at $\delta = 19.48$ and 6.35, in a ratio of approximately 2 to 3; these are assigned to the methylene and methyl hydrogens of the eight peripheral ethyl groups. In order to test whether the absence of signals for coordinated axial ligand was due to paramagnetic or exchange broadening, a large excess of pyridine-*d*₅ was added to the sample. This resulted in formation of the diamagnetic bis(pyridine) complex **6a**. On reexamination of the ¹H NMR spectrum, no signals for free THF, which would have been displaced by the added pyridine, were observed. These results, taken together with the susceptibility data described below, indicate that **5** is four-coordinate Fe(OETAP).

(b) Magnetic Susceptibility of Fe(OETAP) (5). The inverse molar susceptibility of Fe(OETAP) (**5**), determined with a Faraday balance from 4 to 295 K, is shown in Figure 2. Above 40 K, adherence to the Curie-Weiss law is observed, giving an effective magnetic moment, μ_{eff} , of 3.82 μ_{B} . This value compares well with values for μ_{eff} , determined at room temperature, for Fe(TPP) and Fe(Pc) of 4.4^{9a} and 3.85¹⁰ μ_{B} , respectively. In contrast, the effective magnetic moment of the six-coordinate complex, Fe(TPP)(THF)₂, is 5.5 μ_{B} .^{9b}

The possible spin states for a square-planar d⁶ system are *S* = 0, 1, and 2, for which the spin-only magnetic moments are 0, 2.83, and 4.90 μ_{B} , respectively. The effective moment observed for **5** is most consistent with an *S* = 1 spin state in which there is significant coupling with the orbital angular momentum.

As can be seen from the curvature of the low-temperature data in Figure 2, **5** exhibits ferromagnetic interactions below 30 K. We are presently trying to grow diffraction-quality single crystals of **5** in order to understand the structural basis for the ferromagnetic interaction.

(c) Electrochemistry. The six-coordinate bis(pyridine) and bis(1-methylimidazole) adducts, **6a** and **6b**, exhibit reversible oxidations, in dichloromethane, at $E_{1/2} = +0.21$ and -0.06 V vs Ag/AgCl, respectively. These half-wave potentials are over 400 mV positive of the III/II redox couples in the analogous octa-

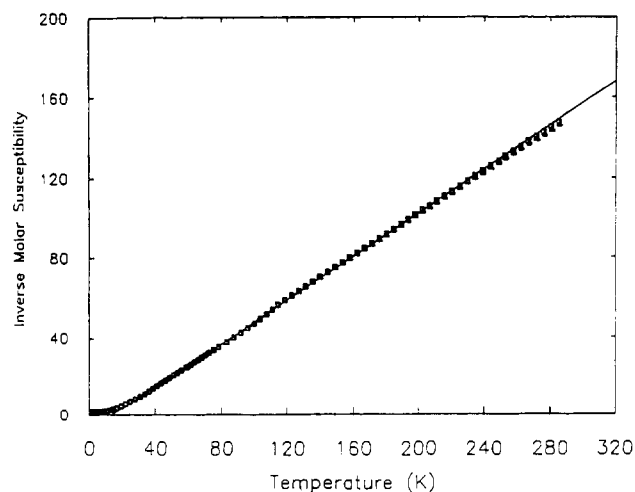


Figure 2. Plot of inverse molar susceptibility versus absolute temperature for microcrystalline Fe(OETAP) (**5**).

ethylporphyrin complexes.¹¹ The shifts in redox potentials are not artifacts of a nonstandard reference as determined by measurements on solutions containing both tetraazaporphyrin and analogous porphyrin complexes. Thus, the tetraazaporphyrin ligand is stabilizing iron(II) relative to the porphyrin ligand. We propose that stabilization of Fe(II) by octaethyltetraazaporphyrin is due to its lower energy π orbitals, which make it a better π acceptor than related porphyrins.¹² Molecular orbital calculations by Gouterman¹³ and, more recently, by Ellis¹⁴ support this proposal.

- (9) (a) Collman, J.; Hoard, J.; Kim, N.; Lang, G.; Reed, C. *J. Am. Chem. Soc.* **1975**, *97*, 2676–2681. (b) Reed, C.; Mashiko, T.; Scheidt, W.; Spartalian, K.; Lang, G. *J. Am. Chem. Soc.* **1980**, *102*, 2302–2306.
 (10) (a) Lever, A. *J. Chem. Soc.* **1965**, 1821–1829 and references therein. (b) Dale, B.; Williams, J.; Johnson, C.; Thorp, T. *J. Chem. Phys.* **1968**, *49*, 3441–3444.

- (11) Brown, G.; Hopf, F.; Meyer, T.; Whitten, D. *J. Am. Chem. Soc.* **1975**, *97*, 5385–5390.
 (12) The higher π acidity of octaethyltetraazaporphyrin compared to octaethylporphyrin is apparent in the CO stretching frequencies of metal carbonyl complexes of these two macrocycles. Greater metal-to-macrocycle back-bonding in the metallotetraazaporphyrin reduces the metal-to-CO back-bonding, as evidenced by higher CO stretching frequencies. $\nu(\text{CO})$ for Ru(OEP)(CO)pyr is reported at 1931 and 1934 cm^{-1} by Ogoshgi et al. (*Bull. Chem. Soc. Jpn.* **1978**, *51*, 2369–2374) and Whitten et al. (*J. Am. Chem. Soc.* **1975**, *97*, 277–281), respectively. $\nu(\text{CO})$ for Ru(OETAP)(CO)pyr is reported at 1962 cm^{-1} (Arnold, H. Personal communication, Stanford University, 1991).
 (13) (a) Weiss, C.; Kobayashi, H.; Gouterman, M. *J. Mol. Spectrosc.* **1965**, *16*, 415–450. (b) Schaffer, A.; Gouterman, M.; Davidson, E. *Theor. Chim. Acta* **1973**, *30*, 9–30.
 (14) Berkovitch-Yellin, Z.; Ellis, D. *J. Am. Chem. Soc.* **1981**, *103*, 6066–6073.

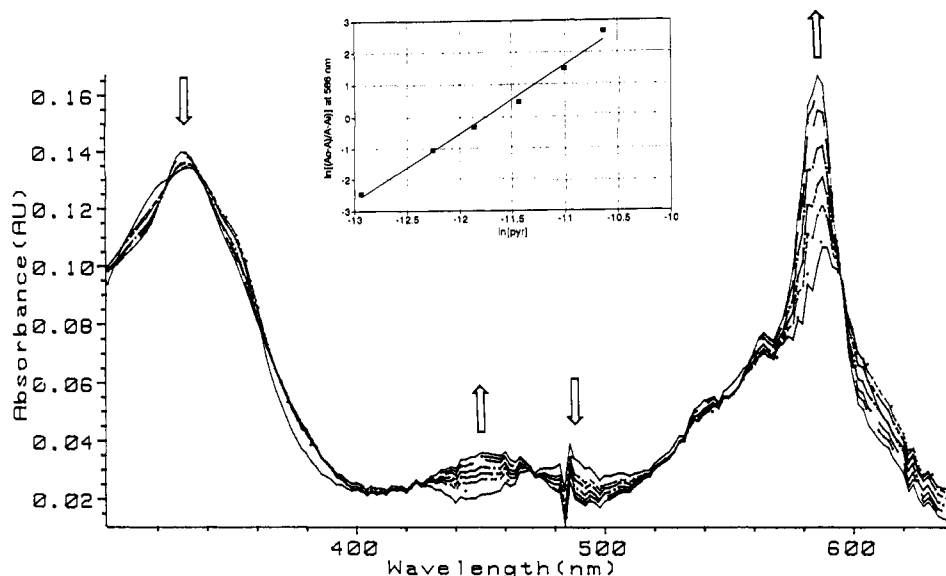
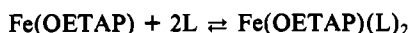


Figure 3. Spectroscopic titration of Fe(OETAP) (5) with pyridine in benzene at 25 °C. $[Fe]_{tot} = 3.0 \times 10^{-6}$ M. $[pyr] = 0-4.0 \times 10^{-5}$ M.

Stronger iron-to-macrocycle back-bonding in **5** raises the effective positive charge on iron compared to ferrous porphyrins. On the basis of electrostatics, one might naively predict that **5** would have a greater affinity for axial ligands than related iron porphyrins; this is confirmed by our results (vide infra).

(d) Axial Ligand Binding to Fe(OETAP) (5). Treatment of dilute ($\approx 1 \times 10^{-6}$ M) benzene solutions of **5** with aliquots of benzene solutions of pyridine or 1-methylimidazole, under rigorously anaerobic conditions, leads to isosbestic changes in the visible spectrum (Figure 3). During the titrations, the cuvette temperature was maintained at 25 ± 0.5 °C.

At relatively high concentrations of nitrogenous base, limiting spectra indicative of Fe(OETAP)(L)₂ (L = 1-MeIm, pyr), low-spin diamagnetic complexes, **6**, were obtained. Plots of $\ln[(A_0 - A)/(A - A_i)]$ vs $\ln[L]^{15}$ at 594 nm had slopes of 2.0 ± 0.1 , unambiguously identifying the reaction as complexation of 2 equiv of axial ligand:



The fact that the changes in the visible spectrum occurred isosbesticly indicates that any monoligand intermediate is present in negligible amounts. Apparently, the equilibrium binding constant for the second ligand must be significantly larger than that for the first. Similar behavior has been reported for four-coordinate iron(II) porphyrins when treated with strong-field ligands (imidazoles and pyridines) and has been attributed to the pairing of electrons in low-lying t_{2g} orbitals of the six-coordinate complex.¹⁶

The equilibrium constant (β) for the ligation of 2 equiv of axial ligand is calculated from the y -intercepts of the plots described above. At 25 °C, these values are determined to be $(3.5 \pm 0.5) \times 10^{11}$ and $(2.0 \pm 0.5) \times 10^{10}$, respectively, for 1-methylimidazole and pyridine. These values are at least 2 orders of magnitude larger than binding constants for related iron(II) porphyrins. Brault and Rougee have reported that deuteroheme, in benzene, coordinates 2 equiv of imidazole¹⁷ or pyridine¹⁸ with binding constants of 4×10^7 and $(1.3 \pm 0.2) \times 10^8$, respectively. As pointed out above, the greater affinity of **5** for axial ligands is

Table I. Crystallographic Data for **8**

(a) Crystal Parameters			
formula	$C_{32}H_{40}N_8ClFe \cdot \frac{1}{2}C_6H_6$	$V, \text{Å}^3$	3463.1 (19)
fw	667.0	Z	4
cryst syst	monoclinic	cryst dimens, mm	$0.32 \times 0.36 \times 0.41$
space group	$P2_1/n$	cryst color	dark red
a, Å	13.324 (4)	$D(\text{calc}), \text{g cm}^{-3}$	1.279
b, Å	19.425 (6)	$\mu(\text{MoK}\alpha), \text{cm}^{-1}$	5.43
c, Å	13.381 (4)	temp, K	297
β , deg	90.09 (2)	$T(\text{max})/T(\text{min})$	1.012
(b) Data Collection			
diffractometer	Nicolet R3m	no. of indpt rflns	4816
monochromator	graphite	R(merge), %	2.03
radiation (λ , Å)	Mo K α	no. of indpt obsd	2651 ($n=5$)
	(0.71073)	rflns, $F_o \geq n\sigma(F_o)$	
2θ scan range, deg	4-46	std rflns	3 std/ 197 rflns
data collected (h,k,l)	$\pm 15,+22,+15$	var in stds, %	~ 3
no. of reflns, collected	5230		
(c) Refinement			
$R(F)$, %	5.74	$\Delta(\rho), \text{e Å}^{-3}$	0.410
$R_w(F)$, %	6.56	N_o/N_v	6.5
$\Delta/\sigma(\text{max})$	0.073	GOF	1.240

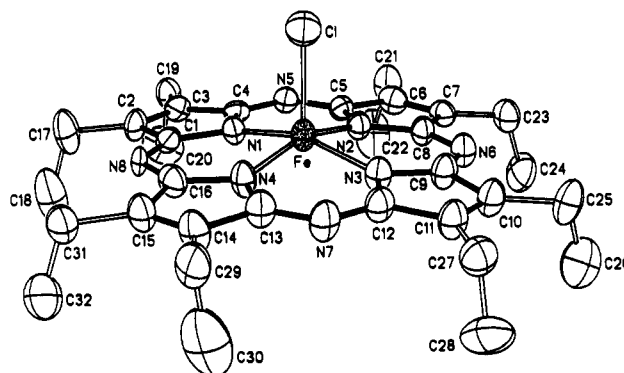


Figure 4. Thermal ellipsoid plot (50% probability) of **8**, Fe(OETAP)Cl.

attributed to a higher effective charge on iron caused by greater iron-to-macrocycle back-bonding. Consistent with this interpretation are the approximately equal affinities of Fe(OETAP)Cl (**8**) and related ferric porphyrins for axial ligands (vide infra). Metal-to-macrocycle back-bonding is much less important for iron(III) than for iron(II).¹⁹

(15) (a) Jaffé, H.; Orchin, M. *Theory and Applications of Ultraviolet Spectroscopy*; Wiley: New York, 1962; pp 578-583. (b) McLees, B.; Caughey, W. *Biochemistry* 1968, 7, 642-652.

(16) (a) Collman, J. *Acc. Chem. Res.* 1977, 10, 265-272. (b) Ellis, P.; Linard, J.; Szymanski, T.; Jones, R.; Budge, J.; Basolo, F. *J. Am. Chem. Soc.* 1980, 102, 1889-1896.

(17) Brault, D.; Rougee, M. *Biochem. Biophys. Res. Commun.* 1974, 57, 654-659.

(18) Brault, D.; Rougee, M. *Biochemistry* 1974, 13, 4591-4597.

Table II. Average Bond Distances (Å) and Angles (deg) for **8** and Related Chloroiron(III) Porphyrins and Phthalocyanines

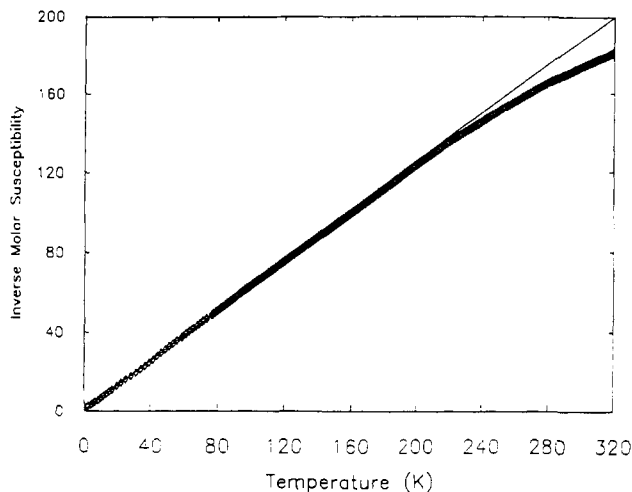
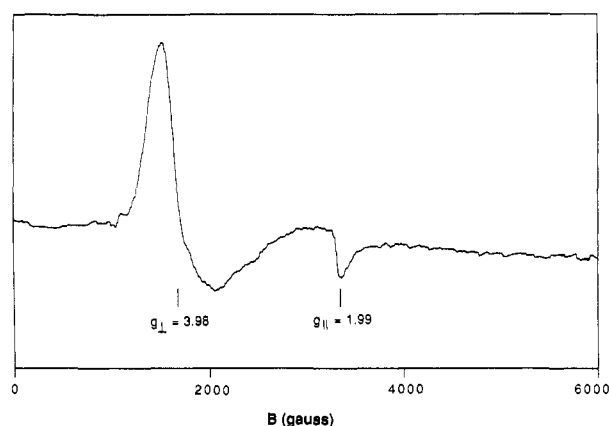
bond or angle	Fe-(OETAP)Cl	Fe-(ProtoP-IX)Cl ²⁰	Fe(Pc)Cl ²¹
Fe-N _p	1.929 (7)	2.067 (6)	1.945 (4)
Fe-Cl	2.278 (2)	2.218 (6)	2.320 (2)
N _p -C _t	1.897 (3)	2.007 (6)	1.871
Fe displacement from N _p plane	0.352 (3)	0.475 (10)	0.30
N _p -αC	1.383 (9)	1.384 (30)	1.381 (5)
αC-βC	1.456 (8)	1.449 (21)	1.448 (5)
βC-βC	1.362 (8)	1.337 (13)	1.392 (5)
αC-bridging atom	1.320 (20)	1.378 (26)	1.317 (5)
αC-bridging atom -αC	121.3 (0.95)	125.95 (1.45)	121.44 (0.32)

Interestingly, when Fe(OETAP) (**5**) is exposed to halogenated hydrocarbons (chloroform), rapid oxidation to Fe(OETAP)Cl is observed. No corresponding reduction product was observed.

Iron(III) Derivatives. (a) X-ray Crystal Structure of Fe(OETAP)Cl (8**).** Diffraction-quality crystals of Fe(OETAP)Cl (**8**) were obtained by slow evaporation of solvent from a benzene/hexane solution over the course of 1 week. The crystal space group is $P2_1/n$, and the unit cell contains four tetraazaporphyrin molecules and two benzene solvate molecules. Crystal parameters and data collection and refinement procedures are given in Table I. The ORTEP diagram, with atomic numbering scheme, is shown in Figure 4. The eight ethyl groups of Fe(OETAP)Cl (**8**) are directed toward the same side of the porphyrin plane, opposite that occupied by the axial chloride ligand. The tetraazaporphyrin core is "domed" very slightly but shows no S_4 , or "ruffling", distortion.

Selected average bond lengths and angles of **8** are compared to those of related chloroiron(III) porphyrin²⁰ and phthalocyanine²¹ complexes in Table II. The average distances between the iron atom and pyrrolic nitrogen atoms (Fe-N_p) and between the macrocycle center and pyrrolic nitrogen atoms (N_p-C_t) are smaller in the tetraazaporphyrin and phthalocyanine complexes than in the porphyrin derivative. Thus, the metal-binding "hole" (distance between transannular pyrrolic nitrogen atoms) in the aza nitrogen-bridged macrocycles is smaller than that of the porphyrin. This is a result of two effects: (1) shorter bond distances between the pyrrolic α-carbon and the bridging nitrogen atoms and (2) smaller bond angles about the bridging nitrogen atoms. Both of these features tend to "squeeze" the pyrrole rings of the tetraazaporphyrin and phthalocyanine complexes closer together than in the porphyrin macrocycle. Due to their smaller "hole" size, tetraazaporphyrins (and phthalocyanines) are stronger σ donors than porphyrins (vide infra).

Despite the smaller "hole" size, the iron atom is displaced less from the tetraazaporphyrin or phthalocyanine plane than it is from the porphyrin plane. Scheidt and Reed²² have shown the intimate relationship between the displacement of iron from the porphyrin plane and the occupancy of the $d_{x^2-y^2}$ orbital (i.e. iron spin state) in a number of five-coordinate iron porphyrins. Large displacements (0.39–0.62 Å) are observed for high-spin ($S = 5/2$) complexes in which the antibonding $d_{x^2-y^2}$ orbital is occupied. Repulsive interactions between the electron in the iron $d_{x^2-y^2}$ orbital and electrons on the pyrrolic nitrogens prevent the iron atom from dropping into the porphyrin plane. This is the case for all chloroiron(III) porphyrins reported to date.^{20,23} For ferric porphyrins in which the $d_{x^2-y^2}$ orbital is unoccupied ($S = 1/2$ or $3/2$)²⁴ or

**Figure 5.** Plot of inverse molar susceptibility versus absolute temperature for microcrystalline Fe(OETAP)Cl (**8**).**Figure 6.** EPR spectrum at 77 K of a frozen glass of Fe(OETAP)Cl (**8**) in toluene. Conditions: [**8**] = 0.011 M, frequency = 9.04 GHz; gain = 3.2×10^5 ; time constant = 1.25 s; modulation amplitude = 20; sweep time = 500 s.

partially occupied (admixed $S = 3/2, 5/2$),²⁵ smaller displacements of iron from the macrocycle plane (0.00–0.30 Å) are observed. The only structurally characterized ferric phthalocyanine exhibits the same relationship between iron spin state and displacement from the macrocycle plane.²¹

The displacement of iron from the tetraazaporphyrin plane in **8** suggests that the $d_{x^2-y^2}$ orbital is unoccupied in this complex, thus allowing the iron to drop closer into the tetraazaporphyrin binding site. Apparently, the smaller "hole" of the tetraazaporphyrin splits the iron d orbitals to a greater extent than does a porphyrin, resulting in a lower spin ($S < 5/2$) complex. We show below, by magnetic susceptibility measurements and Mössbauer and EPR spectroscopies, that Fe(OETAP)Cl (**8**) is an unusual, intermediate-spin ($S = 3/2$) complex. While a number of admixed $S = 3/2, 5/2$ ferric porphyrins²⁵ and phthalocyanines²⁶ have been reported, we are aware of only four examples of pure $S = 3/2$ ferric porphyrins^{24d,27} and phthalocyanines.^{26b}

(19) C-N stretching frequencies of 2120 and 2041 cm^{-1} are reported for $\text{K}_3[\text{Fe}(\text{CN})_6]$ and $\text{K}_4[\text{Fe}(\text{CN})_6] \cdot 3\text{H}_2\text{O}$, respectively, by: Pouchart, C. *The Aldrich Library of FT-IR Spectra*; Aldrich: Milwaukee, WI, 1985; pp 1251–1252. See also: Huheey, J. *Inorganic Chemistry, Principles of Structure and Reactivity*; Harper & Row: New York, 1978; pp 403–411.

(20) Koenig, D. *Acta Crystallogr.* **1965**, *18*, 663–673.

(21) Palmer, S.; Stanton, J.; Jaggi, N.; Hoffman, B.; Ibers, J.; Schwartz, L. *Inorg. Chem.* **1985**, *24*, 2040–2046.

(22) Scheidt, W.; Reed, C. *Chem. Rev.* **1981**, *81*, 543–555.

(23) Hoard, J.; Cohen, G.; Glick, M. *J. Am. Chem. Soc.* **1967**, *89*, 1992–1996.

(24) (a) Collins, D.; Countryman, R.; Hoard, J. *J. Am. Chem. Soc.* **1972**, *94*, 2066–2072. (b) Little, R.; Dymock, K.; Ibers, J. *J. Am. Chem. Soc.* **1975**, *97*, 4532–4539. (c) Scheidt, W.; Haller, K.; Hatano, K. *J. Am. Chem. Soc.* **1980**, *102*, 3017–3021. (d) Summerville, D.; Cohen, I.; Hatano, K.; Scheidt, W. *Inorg. Chem.* **1978**, *17*, 2906–2910.

(25) (a) Reed, C.; Mashiko, T.; Bentley, S.; Kastner, M.; Scheidt, W.; Spartalian, K.; Lang, G. *J. Am. Chem. Soc.* **1979**, *101*, 2948–2958. (b) Masuda, H.; Taga, T.; Osaki, K.; Sugimoto, H.; Yoshida, Z.; Ogoshi, H. *Inorg. Chem.* **1980**, *19*, 950–955. (c) Gismelseed, A.; Bominaar, E.; Bill, E.; Trautwein, A.; Winkler, H.; Nasri, H.; Doppelt, P.; Mandon, D.; Fischer, J.; Weiss, R. *Inorg. Chem.* **1990**, *29*, 2741–2749.

(26) (a) Kennedy, B.; Brain, G.; Murray, K. *Inorg. Chim. Acta* **1984**, *81*, L29–L31. (b) Kennedy, B.; Murray, K.; Zwack, P.; Homborg, H.; Kalz, W. *Inorg. Chem.* **1986**, *25*, 2539–2545.

Table III. Mössbauer Parameters for **8**^a

T, K	site	ΔE_Q , mm/s	δ , mm/s	% area
80	A	3.07 (1)	0.37 (1)	73.8
	B	3.00 (1)	0.19 (1)	26.2
298	A	2.98 (1)	0.28 (1)	74.6
	B	2.90 (1)	0.065 (3)	25.4

^a ΔE_Q (quadrupole splitting) and δ (isomer shift) are relative to iron foil.

Comparison of Fe(OETAP)Cl (**8**) and Sn₄-star-Ni(porphyrine)S₈, the only other structurally characterized tetraazaporphyrin,²⁸ has also proven interesting. The bond distances, bond angles, and "hole" sizes of these two complexes are remarkably similar. Coordination of the four tin atoms by the eight thiolate ligands on the macrocycle periphery does not appreciably alter the macrocycle geometry for Sn₄-star-Ni(porphyrine)S₈.

(b) **Magnetic Susceptibility of Fe(OETAP)Cl (**8**).** Magnetic susceptibilities, measured on a microcrystalline sample with a Faraday balance from 4 to 295 K, indicate a pure $S = 3/2$ spin state for iron in **8**. As can be seen in Figure 5, Curie-Weiss behavior, with an effective magnetic moment ranging from 3.90 to 3.94 μ_B , is observed. This compares to the expected $S = 3/2$ spin-only value of 3.87 μ_B .

As mentioned above, chloroiron(III) porphyrin complexes are invariably $S = 5/2$ spin systems²² while chloroiron(III) phthalocyanine is now believed to be an $S = 3/2, 5/2$ admixed system.²⁶ As discussed above, the strongly σ -donating tetraazaporphyrin ligand induces greater splitting of the iron d orbitals, resulting in a lower spin complex. Scheidt²⁹ has noted the extreme sensitivity of iron spin state to the nature of the tetrapyrrolic macrocycle in complexes of this type.

(c) **EPR Spectra of Fe(OETAP)Cl (**8**).** The EPR spectrum of **8**, Fe(OETAP)Cl, was measured at 77 K for both the microcrystalline powder and a dilute ($\approx 1 \times 10^{-2}$ M) toluene solution (Figure 6). In both cases, a spectrum consistent with an axially symmetric complex was obtained. The large line width of the solid spectrum precluded measurement of g values for that sample, but values of $g_{\perp} = 3.98$ and $g_{\parallel} = 1.99$ were obtained from the spectrum of the frozen solution. Simple theory predicts a value of $g_{\perp} = 4$ for an $S = 3/2$ system in which there is large zero-field splitting.³⁰ Thus, the measured value of $g_{\perp} = 3.98$, strongly supports the $S = 3/2$ assignment for Fe(OETAP)Cl (**8**).

Values of g_{\perp} for related systems reported in the literature include 4.2 for Fe(T(MeO)₃PP)ClO₄,^{27c} 4.67 for Fe(Pc)Cl,²⁶ and 4.75 for Fe(TPP)ClO₄.^{25a} The first of these is reported to be a pure $S = 3/2$ system, while the last two are best characterized as admixed $S = 3/2, 5/2$ systems.

(d) **Mössbauer Spectra of Fe(OETAP)Cl (**8**).** The Mössbauer spectra of ferric porphyrins^{25,27,31} and phthalocyanines^{26,32} have been shown to be quite sensitive to iron spin state. Large quadrupole splittings (ΔE_Q), greater than 2.5 mm/s, have been reported for $S = 3/2$ complexes. Significantly smaller values of ΔE_Q are observed for $S = 1/2$ and $S = 5/2$ complexes (≈ 1.6 – 2.3 and ≈ 0.5 – 1.3 mm/s, respectively).

The Mössbauer spectrum of **8** has been measured on a microcrystalline sample at room temperature (Figure 7a) and at 80

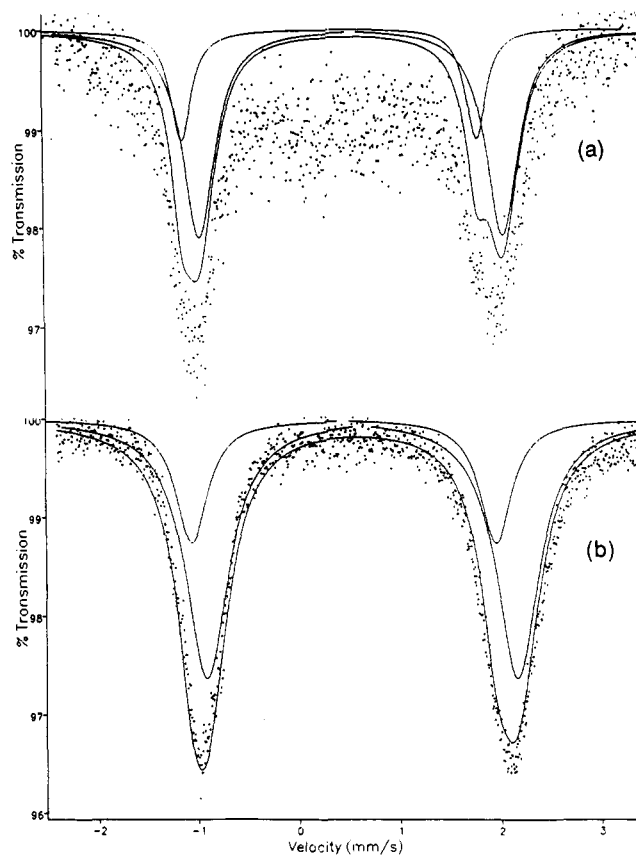


Figure 7. Mössbauer spectra of microcrystalline Fe(OETAP)Cl (**8**) at 298 K (a) and 80 K (b). Velocity values are relative to sodium nitroprusside (subtract 0.257 mm/s to convert to iron metal standard).

K (Figure 7b). As listed in Table III, there are, at both temperatures, two doublets with ΔE_Q of about 3 mm/s with differing isomer shifts (δ). This indicates that there are two iron sites in the crystal, a major component (A) accounting for 75% of the total iron and a minor component (B) accounting for the remainder.

The Mössbauer parameters observed for **8** indicate that both types of iron are in the $S = 3/2$ spin state, consistent with the magnetic susceptibility results. We believe the two iron sites, evident in the Mössbauer spectra of **8**, are due to different local environments for iron, possibly caused by differences in solvation. This material has been crystallized in two forms, a nonsolvate and a half benzene solvate.³³ The possibility of a chemical impurity was ruled out by elemental analysis, and evidence for a magnetic impurity was not seen in either the susceptibility measurements or the EPR spectrum. The possibility of two iron octaethyltetraazaporphyrins being different due to site symmetry within the crystal has been ruled out by the crystal structure.

(e) **Axial Ligand Binding to Fe(OETAP)Cl (**8**).** Treatment of a chloroform solution of Fe(OETAP)Cl (**8**) ($\approx 2 \times 10^{-5}$ M), with aliquots of 1-methylimidazole/chloroform solutions, in a thermostated cell, gave isosbestic changes in the visible spectrum, shown in Figure 8. At relatively high concentrations of 1-methylimidazole (≥ 0.10 M), a limiting spectrum indicative of saturation was obtained. The spectra were analyzed by plotting $\ln [(A_0 - A)/(A - A_f)]$ vs $\ln [1 - \text{MeIm}]$ ¹⁵ at 346, 446, 568, and 684 nm. All four plots were linear with an average slope of 2.0 ± 0.1 , indicating formation of the bis(imidazole) complex, **9**. The equilibrium constant (β), calculated from the y-intercepts of the plots described above, was determined to be $(9.0 \pm 0.5) \times 10^3$ at 25 °C, a value that is surprisingly close to the β of 6.8×10^3 determined by Walker et al.³⁴ for the binding of 2 equiv of 1-MeIm

- (27) (a) Dolphin, D.; Sams, J.; Tsin, T. *Inorg. Chem.* **1977**, *16*, 711–713. (b) Mansuy, D.; Morgenstern-Badarau, I.; Lange, M.; Gans, P. *Inorg. Chem.* **1982**, *21*, 1427–1430. (c) Toney, G.; terHaar, L.; Savrin, J.; Gold, A.; Hatfield, W.; Sangaiah, R. *Inorg. Chem.* **1984**, *23*, 2563–2564.
- (28) Velazquez, C.; Broderick, W.; Sabat, M.; Barrett, A.; Hoffman, B. J. *Am. Chem. Soc.* **1990**, *112*, 7408–7410.
- (29) Geiger, D.; Scheidt, W. *Inorg. Chem.* **1984**, *23*, 1970–1972.
- (30) Drago, R. *Physical Methods in Chemistry*; Saunders: Philadelphia, PA, 1977; Chapter 13.
- (31) Sams, J.; Tsin, T. In *The Porphyrins*; Dolphin, D., Ed.; Academic: New York, 1979; Vol. IV, pp 425–478.
- (32) (a) Hudson, A.; Whitfield, H. *Inorg. Chem.* **1967**, *6*, 1120–1123. (b) Taube, R.; Dreves, H.; Fluck, E.; Kuhn, P.; Brauch, K. Z. *Anorg. Allg. Chem.* **1969**, *364*, 297–315. (c) Dézsi, I.; Balázs, A.; Molnár, B.; Gorobchenko, V.; Lukashovich, I. *J. Inorg. Nucl. Chem.* **1969**, *31*, 1661–1666.

- (33) See compound **8** in the Experimental Section. Evidence for a half benzene solvate and a nonsolvate comes from the X-ray crystal structure and elemental analyses.

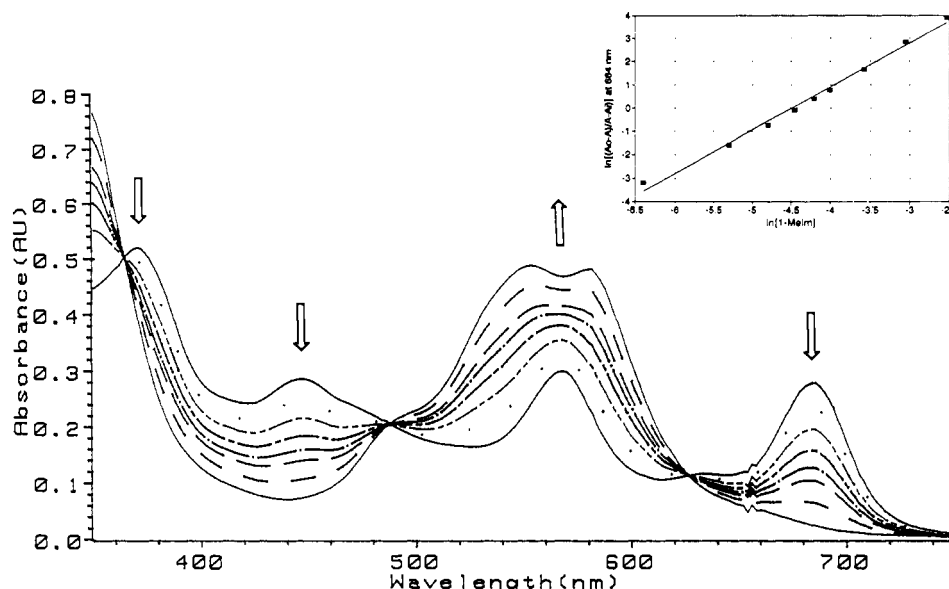


Figure 8. Spectroscopic titration of Fe(OETAP)Cl (8) with 1-MeIm in CHCl_3 at 25 °C. $[\text{Fe}]_{\text{tot}} = 2.1 \times 10^{-5} \text{ M}$. $[1\text{-MeIm}] = 0\text{--}0.14 \text{ M}$.

to chloroiron(III) octaethylporphyrin under identical conditions. The similarity in the equilibrium constants for 1-MeIm binding to iron(III) octaethylporphyrin and octaethyltetraazaporphyrin is in contrast to the dissimilar binding constants for nitrogenous ligands and the iron(II) complexes. Differences between the iron(II) complexes were attributed to differences in the π -accepting properties of the macrocyclic ligands. Since π back-bonding from iron(III) is relatively weak,¹⁹ little difference is expected between the porphyrin and tetraazaporphyrin complexes of iron(III).

Crystals of **9** were deposited by layering hexanes and methanol onto a solution of Fe(OETAP)Cl (8) in 1% 1-methylimidazole/chloroform. This material had an elemental analysis consistent with $[\text{Fe}(\text{OETAP})(1\text{-MeIm})_2]\text{Cl}$. A room-temperature susceptibility of $3.04 \mu_B$, determined by the Evans method, is most consistent with a six-coordinate, low-spin complex.

Interestingly, when benzene (vice chloroform) solutions of Fe(OETAP)Cl are treated with excess 1-MeIm, reduction to Fe(II) occurs, the final product being $\text{Fe}(\text{OETAP})(1\text{-MeIm})_2$ (**6b**). Reduction of iron(III) porphyrins in the presence of a large excess of imidazole has been reported,³⁵ but it is not clear why this should be a facile process for iron(III) tetraazaporphyrins in benzene yet undetected in chloroform.

Conclusion

Tetraazaporphyrins and their metal complexes, for lack of a convenient route to soluble, stable derivatives, are relatively unexplored compared to porphyrins and phthalocyanines. An efficient, general synthesis, reported recently,⁶ removes one obstacle to such studies. The reactivity and structural, magnetic, and electrochemical data presented above for iron tetraazaporphyrins show them to be similar to both porphyrins and phthalocyanines but more like the latter. However, several subtle but important differences have become apparent. Due to a smaller "hole" size, octaethyltetraazaporphyrin is a stronger σ donor than related porphyrins; it splits the d orbitals of a coordinated metal to a greater extent than do porphyrins. For this reason, chloroiron(III) octaethyltetraazaporphyrin is an intermediate-spin ($S = 3/2$) complex, whereas all chloroiron(III) porphyrins reported to date are high spin. In spite of being a stronger σ donor than related porphyrins, octaethyltetraazaporphyrin is better able to stabilize Fe(II) over Fe(III) (as evidenced by the positively shifted III/II redox couple). Stabilization of iron(II) is effected by back-bonding from iron into the low-energy π orbitals of the tetraazaporphyrin.

Metal-to-macrocycle electron transfer raises the effective positive charge on the iron, thus increasing the affinity of Fe(OETAP) (relative to iron(II) porphyrins) for axial ligands. This effect is most pronounced for iron(II), where metal-to-macrocycle back-bonding is most important. Compared to phthalocyanines, tetraazaporphyrins offer the advantage of solubility, which makes them tractable and opens up the possibility of homogeneous catalysis. The unusual properties of tetraazaporphyrins suggest they may have better or unique catalytic properties compared to porphyrins and phthalocyanines. These possibilities are currently being explored.

Experimental Section

General Considerations. Manipulations involving air-sensitive compounds were done inside a Braun MB150 inert-atmosphere glovebox maintained at less than 1 ppm of oxygen. All reagents except iron(II) iodide and unmetallated octaethyltetraazaporphyrin were purchased from Aldrich Chemical Co. Iron(II) iodide was purchased from Strem Chemicals, Inc., while free-base octaethyltetraazaporphyrin was prepared as reported in the literature.⁶ All reagents were of commercial quality and were used as purchased unless noted below. Toluene, benzene, and tetrahydrofuran were distilled from sodium/benzophenone ketyl and degassed with nitrogen for 15 min prior to use. Chloroform was washed with water and then dried over calcium chloride, followed by distillation from phosphorus pentoxide. Column chromatography was done using 150-mesh alumina (Aldrich).

Samples were submitted to either Galbraith Laboratories, Inc., Knoxville, TN, or Oneida Research Services, Inc., Whitesboro, NY (air-sensitive samples), for elemental analyses.

¹H NMR spectra were recorded on a General Electric QE300 spectrometer; chemical shift values are reported relative to tetramethylsilane in the solvent indicated. UV-visible spectra were recorded on a Hewlett Packard 8452A diode array spectrometer while EPR spectra were recorded on a Bruker ER-200 spectrometer, calibrated with DPPH. The cyclic voltammograms were obtained with a standard three-electrode cell using a Bioanalytical Systems CV27 potential source and a Princeton Applied Research 174A potentiostat connected to a Bausch and Lomb/Houston X-Y recorder. The working electrode was a platinum disk, and the auxiliary electrode was a platinum wire. The solvent was dichloromethane containing 0.1 M tetrabutylammonium tetrafluoroborate as the electrolyte. Potentials were measured relative to a standard Ag/AgCl reference. The Mössbauer spectra were obtained on a Ranger Scientific Model MS-900 Mössbauer spectrometer coupled with an IBM microcomputer in the acceleration mode with moving-source geometry at 80 K or room temperature. The resultant spectra were analyzed by a constraint, least-squares fit to Lorentzian-shaped lines.³⁶ The samples were mounted in polyethylene or polypropylene cells. The velocity range was calibrated with sodium nitroprusside, and the isomer shift values were converted to the iron standard by subtracting 0.257 mm/s. The

(34) Walker, F.; Lo, M.-W.; Ree, M. *J. Am. Chem. Soc.* **1976**, *98*, 5552–5560.

(35) (a) Quinn, R.; Nappa, M.; Valentine, J. *J. Am. Chem. Soc.* **1982**, *104*, 2588–2595. (b) Srivatsa, S.; Sawyer, D. *Inorg. Chem.* **1985**, *24*, 1732–1734.

(36) Bancroft, G.; Maddock, A.; Ong, W.; Prince, R.; Stone, A. *J. Chem. Soc. A* **1967**, 1966–1971.

magnetic susceptibilities were measured on 25–50-mg solid samples, between 4 and 295 K, on a computer-controlled Faraday system consisting of a Cahn 2000 microbalance, Applied Magnetics electromagnet, Lake Shore Cryotronics temperature controller, platinum resistance thermometer, and Abbess Instruments cryostat. A Data Translation A/D board and AT computer were used to monitor the microbalance output and temperature readings. The instrument was calibrated with $\text{HgCo}(\text{NCS})_4$.³⁷ The raw data were corrected for the susceptibility of the holder, converted to molar susceptibilities, and corrected for the diamagnetism of the component atoms by Pascal's constants.³⁸ The magnetic moments were calculated as $\mu = 2.828(\chi_M T)^{1/2}$.

X-ray Data Collection and Structure Solution of Fe(OETAP)Cl. Suitable crystals of **8** were grown by slow evaporation of solvent from a benzene/hexane solution at room temperature. A dark red $0.32 \times 0.36 \times 0.41$ mm crystal was mounted on a glass fiber with epoxy cement. Crystal data and collection and refinement details are given in Table I. Of the 5230 reflections collected ($4^\circ \leq 2\theta \leq 46^\circ$), 4816 were independent ($R_{\text{int}} = 2.03\%$) and 2651 were observed with $F_o \geq 5\sigma(F_o)$. Intensity data were not corrected for absorption (low μ , $T_{\text{max}}/T_{\text{min}} = 1.012$).

Iron(II) Octaethylporphyrin (5). A mixture of octaethyltetraazaporphyrin (100 mg), anhydrous iron(II) iodide (100 mg), and 2,6-lutidine (20 drops) was dissolved in a stirred 1/1 tetrahydrofuran/toluene mixture (50 mL) at the reflux temperature in an inert-atmosphere glovebox maintained at less than 1 ppm of O_2 . Within 4 h no unmetallated tetraazaporphyrin was present, as shown by UV-visible spectroscopy. The cooled solution was passed through a column (2-cm diameter \times 4-cm length) of neutral alumina in order to remove any iron salts. The column was washed with 50 mL of the same solvent mixture. Reduction of the solvent volume under vacuum caused dark purple-black crystals to form. These were collected by vacuum filtration, washed with hexanes, and dried under vacuum (100 °C, 10 μmHg , 12 h) to yield 100 mg (98%) of needles. This material is extremely oxygen sensitive. UV-visible (C_6H_6): $\lambda_{\text{max}} = 339, 427, 474$ (sh), 489, 537 (sh), 561 (sh), 590, 659 nm (sh). $^1\text{H NMR}$ (C_6D_6): $\delta = 19.48$ (br), 6.35 (br). Anal. Calcd for $\text{C}_{32}\text{H}_{40}\text{N}_8\text{Fe}$: C, 64.87; H, 6.80; N, 18.90. Found: C, 64.77; H, 6.55; N, 18.62.

Iron(II) Octaethyltetraazaporphyrin Bis(pyridine) (6a). A suspension of iron(II) octaethyltetraazaporphyrin (20 mg) in benzene (10 mL) was treated with pyridine (5 drops). The mixture immediately turned deep red, and all solids quickly dissolved. Removal of the solvent and recrystallization of the resulting residue by vapor diffusion of hexane into a benzene solution of the residue gave 20 mg ($\approx 100\%$) of pure product. UV-visible (1% $\text{C}_5\text{H}_5\text{N}/\text{C}_6\text{H}_6$): $\lambda_{\text{max}} = 332, 458, 541, 564$ (sh), 586 nm. $^1\text{H NMR}$ (C_6D_6 , 30 °C): $\delta = 4.09$ (br, 16 H), 2.06 (t, 24 H). $^1\text{H NMR}$ (C_7D_8 , -40 °C): $\delta = 4.35$ (t, 2 H), 4.03 (q, 16 H), 3.87 (t, 4 H), 2.25 (d, 4 H), 2.03 (t, 24 H). Anal. Calcd for $\text{C}_{42}\text{H}_{50}\text{N}_{10}\text{Fe}$: C, 67.01; H, 6.96; N, 18.61. Found: C, 67.23; H, 10.05; N, 18.49.

Iron(II) Octaethyltetraazaporphyrin Bis(1-methylimidazole) (6b). A suspension of iron(II) octaethyltetraazaporphyrin (20 mg) in benzene (10 mL) was treated with 1-methylimidazole (5 drops). The mixture immediately turned deep royal purple, and all solids quickly dissolved. The solvent and excess 1-methylimidazole were removed under vacuum. Crystallization of the resulting residue by vapor diffusion of hexane into a benzene solution of the tetraazaporphyrin gave 20 mg ($\approx 100\%$) of pure product. UV-visible (C_6H_6): $\lambda_{\text{max}} = 315$ (sh), 333, 491, 550 (sh), 574 (sh), 590 nm. $^1\text{H NMR}$ (C_6D_6): $\delta = 4.02$ (q, 16 H), 3.45 (s, 2 H), 2.03 (t, 24 H), 0.30 (s, 2 H), 0.26 (s, 6 H). One of the H's on the coordinated 1-MeIm could not be found in the spectrum. Anal. Calcd for $\text{C}_{40}\text{H}_{52}\text{N}_{12}\text{Fe}\cdot\text{H}_2\text{O}$: C, 62.00; H, 7.02; N, 21.69. Found: C, 62.22; H, 6.73; N, 21.65.

Iron(III) Octaethyltetraazaporphyrin μ -Oxo Dimer (7). A solution of 20 mg of crude iron(II) tetraazaporphyrin (**5**) in 1/1 tetrahydrofuran/toluene, prepared as described above, was stirred in air for 1 h. The resulting solution, diluted with 50 mL of CH_2Cl_2 , was washed twice with 50 mL of 10% aqueous NaOH in a separatory funnel. The resulting deep blue solution was chromatographed on basic alumina using $\text{CH}_2\text{Cl}_2 \rightarrow 1/1 \text{CH}_2\text{Cl}_2/\text{CHCl}_3$ as eluent. A single blue band was isolated. Removal of the solvent and recrystallization of the residue by vapor diffusion of hexane into a benzene/methanol solution of the tetraazaporphyrin gave 20 mg ($\approx 100\%$) of the desired product as a solvate. This material proved to be very sensitive to trace acid in the solvent; all solvent should be passed through a column of basic Al_2O_3 . UV-visible (CHCl_3): $\lambda_{\text{max}} = 351, 579$ (sh), 612 nm. $^1\text{H NMR}$ (C_6D_6): $\delta = 6.59$ (q, 16 H), 5.59 (q,

16 H), 1.80 (t, 48 H). Anal. Calcd for $\text{C}_{64}\text{H}_{80}\text{N}_{16}\text{Fe}_2\text{O}\cdot\frac{1}{2}\text{C}_6\text{H}_6\cdot 2\text{CH}_3\text{OH}$: C, 63.54; H, 7.03; N, 17.18. Found: C, 63.70; H, 6.80; N, 17.16.

Chloroiron(III) Octaethyltetraazaporphyrin (8). Method 1. A solution of 80 mg of crude iron(II) tetraazaporphyrin (**5**) in 1/1 tetrahydrofuran/toluene, prepared as above, was stirred in air for 1 h. The resulting solution, diluted with 100 mL of CH_2Cl_2 , was washed twice with 100 mL of 1.2 M aqueous HCl in a separatory funnel. The resulting deep red solution was dried over Na_2SO_4 and filtered, and the filtrate was reduced on a rotary evaporator to a microcrystalline solid. The solid was next chromatographed on acidic alumina using $\text{CH}_2\text{Cl}_2 \rightarrow 1/1 \text{CH}_2\text{Cl}_2/\text{CHCl}_3$ as eluent. A single deep red band was isolated. Removal of the solvent and recrystallization of the residue by slow evaporation of the solvent from a hexane/benzene solution of the tetraazaporphyrin gave 80 mg ($\approx 100\%$) of the pure product, as a half benzene solvate. UV-visible (CHCl_3): $\lambda_{\text{max}} = 316, 370, 446, 566, 684$ nm. $^1\text{H NMR}$ (C_6D_6): $\delta = 36.74$ (br, 8 H), 13.08 (br, 8 H), 4.84 (br, 24 H). $^1\text{H NMR}$ (CDCl_3): $\delta = 38.76$ (br, 8 H), 15.29 (br, 8 H), 4.06 (br, 24 H). Anal. Calcd for $\text{C}_{32}\text{H}_{40}\text{N}_8\text{FeCl}\cdot\frac{1}{2}\text{C}_6\text{H}_6$: C, 63.02; H, 6.50; N, 16.80. Found: C, 62.47; H, 6.42; N, 16.71. In some instances, microcrystals formed which, by elemental analysis, proved to be nonsolvates. Anal. Calcd for $\text{C}_{32}\text{H}_{40}\text{N}_8\text{FeCl}$: C, 61.20; H, 6.42; N, 17.84. Found: C, 61.04; H, 6.19; N, 17.70.

Method 2. A solution of 10 mg of pure iron(II) octaethyltetraazaporphyrin in 10 mL of toluene was mixed with a solution of 50 mg of silver(I) tetrafluoroborate in 10 mL of toluene in an inert-atmosphere glovebox maintained at less than 1 ppm of O_2 . Reaction was indicated by an immediate color change. This mixture was allowed to stir for 30 min and was then filtered through a packed Celite pad. The Celite pad was washed with an additional 10 mL of toluene, and the washings were combined with the original filtrate. A fine precipitate of silver was observed on the Celite pad. The toluene was removed from the solution under vacuum, and the residue was next dissolved in a solution of 100 mg of benzyltrimethylammonium chloride in 10 mL of CH_2Cl_2 . This mixture was stirred for 15 min and then filtered through a packed Celite pad. The Celite pad was washed with 5 mL of CH_2Cl_2 , and the combined filtrate and washings were reduced under vacuum. The resulting residue was crystallized as in method 1, yielding 8 mg ($\approx 100\%$) of product which proved to be identical, on the basis of elemental analysis and UV-visible and $^1\text{H NMR}$ spectroscopies, to the Fe(OETAP)Cl produced by method 1.

Chloroiron(III) Octaethyltetraazaporphyrin Bis(1-methylimidazole) (9). A solution of 20 mg of chloroiron(III) octaethyltetraazaporphyrin in 10 mL of chloroform was treated with 5 drops of 1-methylimidazole. The mixture immediately turned deep royal purple. Solvent choice is critical; Fe(OETAP)Cl in benzene is reduced to Fe(OETAP)(1-MeIm)₂ on the addition of excess 1-MeIm. Hexane vapor was allowed to diffuse into this solution, resulting in the formation of crystals. These were collected by vacuum filtration, washed liberally with benzene, and dried under vacuum to give 20 mg ($\approx 95\%$) of pure product. UV-visible (0.10 M 1-MeIm/ CHCl_3): $\lambda_{\text{max}} = 331, 348, 488$ (sh), 532, 581 nm. $^1\text{H NMR}$ (0.10 M 1-MeIm/ CDCl_3): $\delta = 17.07$ (br, 6 H), 11.30 (br, 16 H), -0.31 (br, 24 H). One of the H's on the coordinating 1-MeIm could not be found in the spectrum. Anal. Calcd for $\text{C}_{40}\text{H}_{52}\text{N}_{12}\text{FeCl}$: C, 60.64; H, 6.62; N, 21.22. Found: C, 60.24; H, 6.39; N, 21.07.

Acknowledgment. We thank Drs. Joel Miller and Gordon Yee for obtaining the magnetic susceptibility data on iron(II) octaethyltetraazaporphyrin (**5**) and the initial susceptibility data on chloroiron(III) octaethyltetraazaporphyrin (**8**), Prof. Graham Cheek for assistance with the cyclic voltammetry, and Prof. Rinaldo Poli for obtaining the EPR spectra. Helpful discussions with all of the above are gratefully acknowledged. Financial support was provided by the Naval Academy Research Council, the Army Medical Bioengineering Research and Development Laboratory (Mrs. Karen L. Fritz) under the auspices of the U.S. Army Research Office Scientific Services Program, administered by Battelle, and the donors of the Petroleum Research Fund, administered by the American Chemical Society. The computer time for the fitting of the Mössbauer spectra was completely supported by The Catholic University Computer Center.

Supplementary Material Available: Tables of atomic coordinates and isotropic thermal parameters, bond lengths, bond angles, anisotropic thermal parameters, H atom coordinates and isotropic thermal parameters, and susceptibility data (9 pages); a listing of observed and calculated structure factors (8 pages). Ordering information is given on any current masthead page.

(37) O'Connor, C.; Sinn, E.; Cukauskas, E.; Deaver, B. *Inorg. Chim. Acta* 1979, 32, 29–32.

(38) Earnshaw, A. *Introduction to Magnetochemistry*; Academic: New York, 1968.